Hunting Axion and Dark Photon Using Quantum Metrology

Yifan Chen

ITP-CAS

20 November 2021,

2021 Shanghai Particle Physics and Cosmology Symposium, TDLI, Shanghai

Axion/Axion-like Particle

- Hypothetical pseudoscalar initially motivated by strong CP problem:
  Neutron electric dipole $|\bar{\theta}|10^{-16}$ **e.cm is smaller than** 10^{-26} **e.cm.**

  $$\bar{\theta} = \theta_{\rm QCD} + \arg\,\det M_u M_d, \qquad \text{Fine tuning!}$$

  Why is $\bar{\theta}$ so small? Why  instead of ?
  Solution: introducing an **dynamical** field with effective potential

  $$V \sim -m_\Phi^2 f_\Phi^2 \cos(\bar{\theta} + \frac{\Phi}{f_\Phi}).$$

  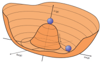

- Extra dimension predicts a wide range of axion mass.
  Dimensional reduction from higher form fields:
  e.g. $A^M(5D) \to A^\mu(4D) + \Phi(4D)$.

- Cold dark matter candidate with wave-like behavior:

  $$\Phi(x^\mu) \simeq \Phi_0(\mathbf{x}) \cos \omega t; \qquad \Phi_0 \simeq \frac{\sqrt{\rho}}{m_\Phi}; \qquad \omega \simeq m_\Phi.$$

  Other candidates: dilaton, dark photon, massive graviton.

Axion Coupling to the Standard Model

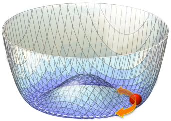

- **Axion Fermion coupling**: $\partial_\mu \Phi \bar{\psi} \gamma^\mu \gamma_5 \psi / f_\Phi$,
  non-linearization of a chiral global symmetry $\sim \partial_\mu \Phi J_5^\mu / f_\Phi$.
  Stellar cooling, **DM wind/gradient**.

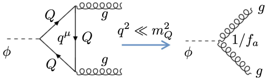

- **Axion Gluon coupling**: $\mathcal{C}_g \Phi \mathrm{Tr}\, G_{\mu\nu} \tilde{G}^{\mu\nu} / f_\Phi$,
  generated from anomaly/triangle loop diagram.
  Oscillating EDM.

- **Axion Photon coupling**: $\mathcal{C}_\gamma \Phi F_{\mu\nu} \tilde{F}^{\mu\nu} / f_\Phi$,
  from mixing with neutral π_0.
  Photon conversion to axion, **inverse Primakoff**, birefringence.

Oscillating field value $\rightarrow$ oscillating observables in standard model sector.

Inverse Primakoff and Haloscope [P.Sikivie 83']

$$\nabla \times \mathbf{B} = \partial_t \mathbf{E} + \mathbf{J} - g_{\Phi\gamma} \left(\mathbf{E} \times \nabla \Phi - \mathbf{B}_0 \partial_t \Phi \right).$$

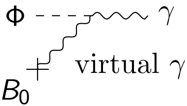

- Inverse Primakoff: $\mathbf{J}_{\rm eff}(t) = g_{\Phi\gamma} \mathbf{B}_0 \partial_t \Phi$.
- Cavity haloscope: $\left(\partial_t^2 + \gamma \partial_t + \omega_c^2\right) \mathbf{E}_{\rm c} = \partial_t \mathbf{J}_{\rm eff}(t)$.
- Static $\mathbf{B_0}$ and resonant when $\omega_c = m_\Phi \sim V^{-1/3} \sim \mathcal{O}(1)$ GHz.

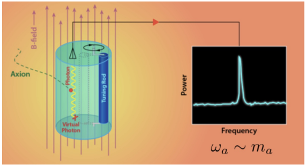

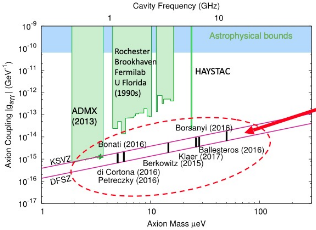

Classical "post inflation" axion window: fine tuning of Θ not required for axions to make up 100% of observed dark matter

e.g. ADMX, CAPP, HAYSTACK

Resonant Detection for Lower m_Φ

- Resonant LC circuit [P.Sikivie et al 14']: $m_\Phi = \omega_{\rm LC} = \frac{1}{\sqrt{LC}}$.

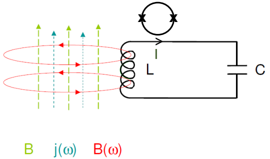

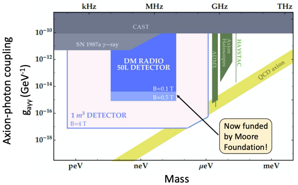

Assumptions: T=10 mK, Q=10^6, 3.5 year integration time, quantum-limited readout

- Resonant SRF Cavity with AC B_0 [Berlin et al 19']

$$\partial_t \mathbf{B}_0 = i\omega_0 \mathbf{B}_0, \quad \omega_1 - \omega_0 = m_\Phi.$$

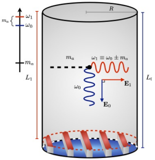

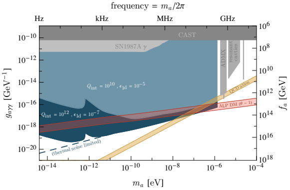

$Q_{\rm int} \equiv \omega/\gamma > 10^{10}$ due to the superconducting nature.

Quantum Noise Limit for EM Resonant Detection

- **Standard quantum limit for power law detection**: [Chaudhuri, Irwin, Graham, Mardon 18']

Noise PSD: resonant intrinsic noise $S_{\rm int}$ + flat readout noise $S_{\rm r}$.

- Sensitivity to $S_{\rm sig}$ and $S_{\rm int}$ is the same.

  SNR^2 $\propto$ range where
  $S_{\rm int}$ dominates over $S_{\rm r}$.

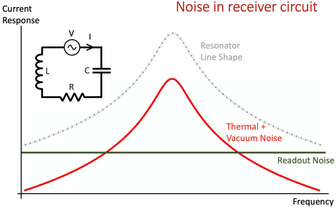

$S_{\rm int} \propto$ Cauchy distribution

- **Beyond quantum limit**:

  Squeezing $S_{\rm r}$, e.g., HAYSTACK.

  Increasing the sensitivity to $S_{\rm sig}$, e.g., white light cavity in optomechanics/GW detection [Miao, Ma, Zhao, Chen 15'].

Dipole Couplings and Spin Precession

Dipole coupling: $H \propto \vec{\mathcal{O}} \cdot \vec{\sigma}_\psi$.

Effective 'magnetic field' $\vec{\mathcal{O}}$ causes precession of the fermions' spin $\vec{\sigma}_\psi$.
[Graham, Rajendran, Budker et al]

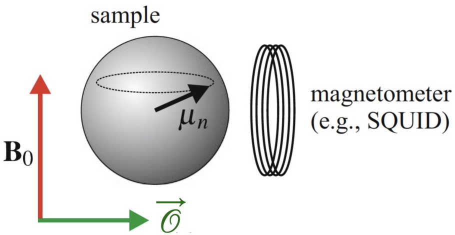

E.g., NMR (Casper) , spin-based amplifiers [Min Jiang's talk], magnon $\cdots$

Vector-like signals:

- **Axion gradient**: $\partial_\mu \Phi \bar{\psi}\gamma^\mu\gamma^5\psi \to \vec{\mathcal{O}}_\Phi = \vec{\nabla}\Phi \propto \vec{\epsilon}_0$.
- **Dark photon with dipole couplings**:

$$V_{\mu\nu}\bar{\psi}\sigma^{\mu\nu}\psi \to \vec{\mathcal{O}}_{\rm MDM} = \vec{\nabla} \times \vec{V} \propto \vec{\epsilon}_{R/L};$$

$$V_{\mu\nu}\bar{\psi}\sigma^{\mu\nu} i\gamma^5\psi \to \vec{\mathcal{O}}_{\rm EDM} = \partial_0 \vec{V} - \vec{\nabla} V^0 \propto \begin{cases} \vec{\epsilon}, & m \gg |p|, \\ \vec{\epsilon}_{R/L}, & m \ll |p|. \end{cases}$$

General Axion & Dark Photon Background

- **Cosmological isotropic background** [CaB, Dror et al 21']:

  Thermal freeze out,
  Topological defect decay,
  Parametric resonance/tachyonic instability of inflaton,
  ...

- **Sources from a specific direction**:

  Cold stream of dark matter,
  Emissions from superradiant clouds.
  Dipole radiations from U(1)' charged binaries
  ...

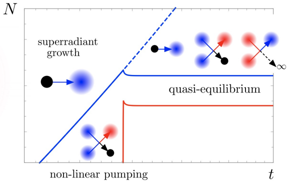

[Baryakht et al 20']

Broad spectrum with potential **anisotropy or macroscopically polarization**.

A Network of Sensors?

- **Beyond quantum limit of the sensitivity/scan rate?**

Axion Haloscope Array With $\mathcal{PT}$ Symmetry

arxiv: 2103.12085, YC, MY.Jiang, Y.Ma, J.Shu, Y.Yang.

- **Identification of the macroscopic and microscopic nature?**

Dissecting Axion and Dark Photon

with A Network of Vector Sensors

arxiv: 2111.06732, YC, M.Jiang, J.Shu, X.Xue, Y.Zeng.

White Light Cavity [X.Li, M.Goryachev, Y.Ma et al 20']

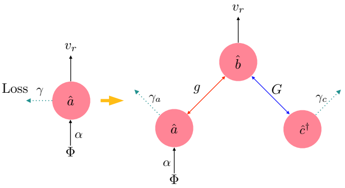

Single Cavity Design

Detector Design with $\mathcal{PT}$ symmetry

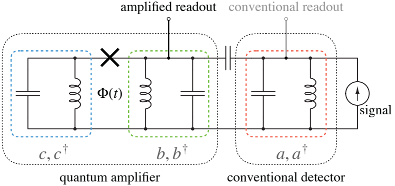

Probing mode: $\hbar\alpha(\hat{a} + \hat{a}^\dagger)\Phi$

- **Beam-splitting**: $\hbar g(\hat{a}\hat{b}^\dagger + \hat{a}^\dagger\hat{b})$.
- **Non-degenerate parametric interaction**: $\hbar G(\hat{b}\hat{c} + \hat{b}^\dagger\hat{c}^\dagger)$.
- **$\mathcal{PT}$-symmetry ($\hat{a} \leftrightarrow \hat{c}^\dagger$)** **emerges** when $g = G$.

$$(\dot{\hat{a}} + \dot{\hat{c}}^\dagger) = -i(g - G)\hat{b} - i\alpha\Phi + \cdots ;$$
$$\dot{\hat{b}} = -\gamma_r\hat{b} - ig(\hat{a} + \hat{c}^\dagger) + \cdots .$$

- Coherent cancellation leads to **double resonance**.
  $S_{\rm sig}$ is largely enhanced when $g \gg$ **intrinsic dissipation** γ:

$$S_{\rm sig}^{\rm WLC}(\Omega) = \frac{2\gamma_r\alpha^2 S_\Phi(\Omega)}{(\gamma+\gamma_r)^2 + \Omega^2}\left(\frac{g^2}{\gamma^2+\Omega^2}\right).$$

Readout coupling γ_r

Binary Tree Haloscope and Physics Reach

- $\mathrm{SNR}^2 \propto$ range where $S_{\rm int}$ dominates over $S_{\rm r}$ $\propto 2^n \left(\frac{g}{\gamma n_{\rm occ}}\right)^{\frac{2n}{2n+1}}$, where $g/\gamma \to Q_{\rm int}$.

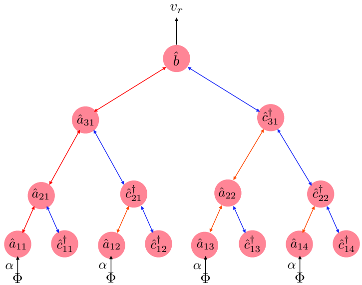

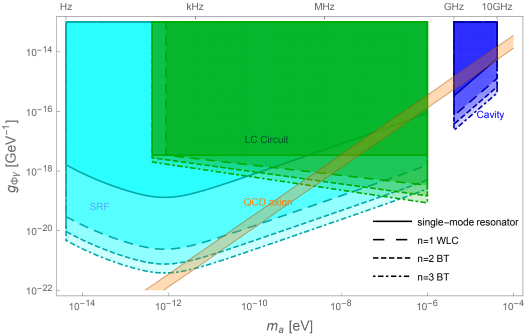

- High $Q_{\rm int}$ of SRF with BT can cover $m_\Phi >$ kHz QCD axion dark matter potentially.

- Strong **robustness** from $\mathcal{PT}$**-symmetry** $\hat{a}_{ij} \leftrightarrow \hat{c}^\dagger_{ij}$.

Vector Sensor Interferometry For Isotropic Backgrounds

A pair of vector sensors separated by a baseline $\vec{d}$:

$$\mathcal{F}(\vec{d}, \vec{l}_I, \vec{l}_J) \propto \langle (\vec{\mathcal{O}}(t, \vec{x}_I) \cdot \hat{l}_1)(\vec{\mathcal{O}}(t, \vec{x}_J) \cdot \hat{l}_2) \rangle, \qquad \vec{d} \equiv \vec{x}_I - \vec{x}_J.$$

For isotropic sources $f_{\rm iso}(p, \hat{\Omega}) = \frac{f_{\rm iso}(p)}{4\pi p^2}$:

- Dipole correlation for each mode of $\vec{\epsilon}$ at $d = 0$.

$$\mathcal{F} \propto \hat{l}_I \cdot \hat{l}_J = \cos\theta_{IJ}$$

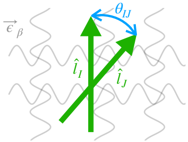

- Finite baseline distinguishes $\vec{\epsilon}_0$ from $\vec{\epsilon}_{R/L}$ at $\xi \equiv p\,d \approx 4$.

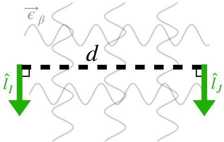

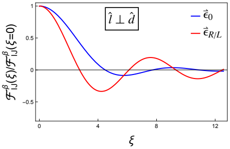

- A twisted setup can identify the macroscopic circular polarization from a parity-violating production.

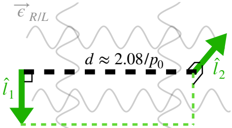

Localization

Sources from a specific direction $f_{\rm str}(p,\hat{\Omega}) = \frac{f_{\rm str}(p)}{p^2}\,\delta^2(\hat{\Omega}-\hat{\Omega}_0)$:

- Short baseline limit with $d=0$:
  The optimal arrangements of the sensors are the same for $\vec{\epsilon}_0$ and $\vec{\epsilon}_{R/L}$, reaching $\sigma_\Omega \approx 1/\mathrm{SNR}$.

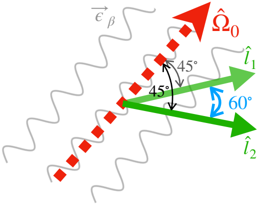

- Long baseline limit:
  The sensitive directions should overlap with the signals as much as possible with $\sigma_\theta \approx 1/(\mathrm{SNR}\,p\,d)$.

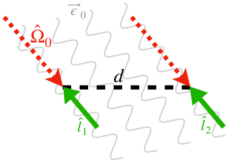

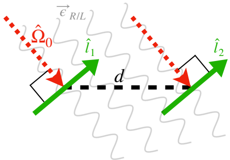

Multi-messenger astronomy with **GNOME**!

Summary

- **Multi-mode resonator with $\mathcal{PT}$ symmetry** can go far beyond the quantum limit with effective squeezing factor $Q_{\rm int}/n_{\rm occ}$.
  The SRF haloscope, with **a high** $Q_{\rm int}$, can probe most of the QCD axion mass window.
- **Correlations of vector sensor array** can identify the macroscopic property and the microscopic nature of the bosonic background;
- **Quantum metrology** can play huge rules in fundamental physics!

Thank you!

Appendix

Oscillating Ultralight Scalar Background

- Non-relativistic light bosons behave as **coherent wave** when the occupation number is large:

$$\Phi(x^\mu) \simeq \Phi_0(\mathbf{x}) \cos \omega t; \qquad \Phi_0 \simeq \frac{\sqrt{\rho}}{m_\Phi}; \qquad \omega \simeq m_\Phi.$$

- Cold dark matter candidate, wave-like when $m_\Phi < 1$ eV.

- **Oscillating field value: physical observables in standard model sector oscillate as well**:
  Dilaton: coupling constant, mass...
  Axion: EDM, chiral dispersion of photon...

- **The interactions with SM are suppressed by high scale.**

- **Amplifications of the signals:**
  Tabletop experiments on earth: $\rho_{\rm DM} \sim 0.4~\mathrm{GeV/cm^3}$;
  Astrophysical: **larger** ρ_Φ, e.g., galaxy center or near Kerr black hole.

Axion QED: Inverse Primakoff Effect

- Axion-electrodynamics modifies Maxwell equations:

$$\nabla \cdot \mathbf{E} = \rho - g_{\Phi\gamma} \mathbf{B} \cdot \nabla \Phi$$
$$\nabla \times \mathbf{B} = \partial_t \mathbf{E} + \mathbf{J} - g_{\Phi\gamma} \left(\mathbf{E} \times \nabla \Phi - \mathbf{B} \partial_t \Phi \right)$$

- Neglecting spatial derivative, background $\mathbf{B}_0$ and **axion dark matter** Φ leads to **effective current**

$$J_{\rm eff}(t) \sim g_{\Phi\gamma} B_0(t) \sqrt{\rho_{\rm DM}} \cos m_\Phi t.$$

- Inverse Primakoff effect: the conversion of axion to an **oscillating EM field** under background $\mathbf{B}_0$.

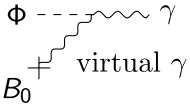

Misalignment Production of QCD Axion

- For QCD axion, $m_\Phi f_\Phi \sim \Lambda^2_{\rm QCD}$ predicts a **thin line in the parameter space**.
- Cosmological parameter: initial misalignment angle $\theta_i \equiv \Phi_i / f_\Phi$.

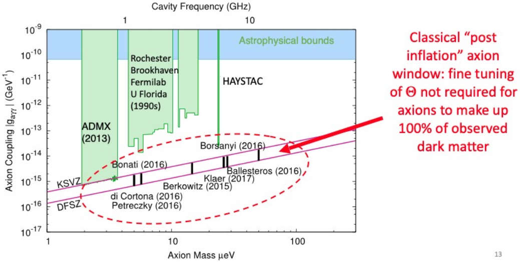

- Assuming $\theta_i \sim 1$ leads to the most natural region of QCD axion dark matter $m_\Phi \sim 10^{-6}\mathrm{eV} \sim$ GHz.
- Different cosmological evolutions can still provide a viable dark matter candidate in other region, e.g., PQ symmetry broken before inflation.

Property of Axion Dark Matter

Galaxy formation: virialization gave $\sim 10^{-3}c$ velocity fluctuation, thus kinetic energy $\sim 10^{-6} m_\Phi c^2$ currently.
Effectively coherent wave:

$$\Phi(\vec{x}, t) = \frac{\sqrt{2\rho_\Phi}}{m_\Phi} \cos\left(\omega_\Phi t - \vec{k}_\Phi \cdot \vec{x} + \delta_0\right).$$

- Bandwidth: $\delta\omega_\Phi \simeq m_\Phi \left\langle v_{\rm DM}^2 \right\rangle \simeq 10^{-6} m_\Phi$, $Q_\Phi \simeq 10^6$.
- Correlation time: $\tau_\Phi \simeq \mathrm{ms}\, \frac{10^{-6}\mathrm{eV}}{m_\Phi}$.
  Power law detection is used to make integration time longer than τ_Φ.
- Correlation length: $\lambda_d \simeq 200\ \mathrm{m}\frac{10^{-6}\mathrm{eV}}{m_\Phi} \gg \lambda_c = 1/m_\Phi$.
  Sensor array can be used within λ_d.

Superradiance and Gravitational Atom

- **Rotational and dissipational medium** can amplify the wave around. [Zeldovichi 72']
- **Superradiance**: the wave-function is exponentially amplified from extracting BH rotation energy when $\lambda_c \simeq r_g$. [Penrose, Starobinsky, Damour et al]
- **Gravitational bound state** around BH:

$$\Phi(x^\mu) = e^{-i\omega t} e^{im\phi} S_{lm}(\theta) R_{lm}(r),$$

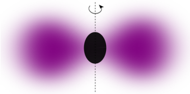

- Stringent Constraint using EHT data [EHT 21']:

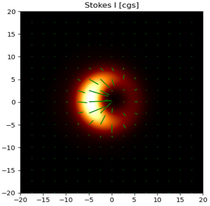

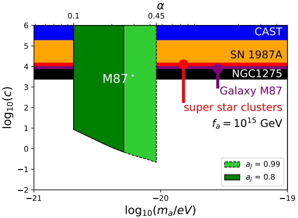

[YC, Liu, Lu, Mizuno, Shu, Xue, Yuan, Zhao 21']

Axion Wave from Saturating Axion Cloud

- **Self interaction saturating phase where $\Phi_{\mathbf{max}} \simeq f_\Phi$.** [Yoshino, Kodama 12', Baryakht et al 20'].

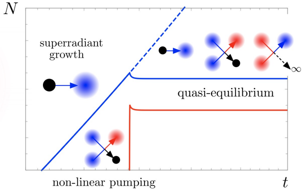

- Two level state with 2, 1, 1 and 3, 2, 2. Annihilations between 3, 2, 2 lead to **'ionized' axion wave** with velocity $v \sim \alpha/6$:

$$B_\Phi \simeq 3 \times 10^{-24}\ \mathrm{T} \times \mathcal{C}_N \left(\frac{\alpha}{0.1}\right)^4 \left(\frac{1\mathrm{kpc}}{r}\right), \qquad \text{[Baryakht et al 20']}$$

- For BH $\sim 10 M_\odot$, superradiance happens for $m_\Phi \sim 100$ Hz axion. **Axion gradient/paraphoton signal is expected!**

- **Localization of the source** with three transverse directions of dipole sensors and long baseline such that $\delta\theta \propto \lambda_c/d$.

  Multi-messenger astronomy with GNOME!

Resonator Chain Haloscope

- Generalization to chain detector:

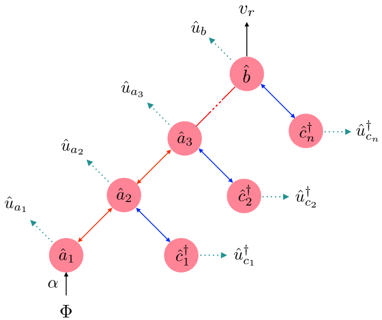

- $\mathcal{PT}$-invariant mode: $\hat{A}_i \equiv \hat{a}_i + \hat{c}_i^\dagger$.

$$\dot{\hat{A}}_1 = -i\alpha\Phi + \cdots\,,$$
$$\dot{\hat{A}}_i = -ig\hat{A}_{i-1} + \cdots\,,$$
$$\dot{\hat{b}} = -\gamma_r\hat{b} - ig\hat{A}_n.$$

$n+1$**-times resonance!**

- The whole Hamiltonian is explitly $\mathcal{PT}$ **broken**.

- $S_{\rm sig}$ is n-times enhanced:

$$S_{\rm sig}^{\rm RC}(\Omega) = \frac{2\gamma_r\alpha^2 S_\Phi(\Omega)}{(\gamma+\gamma_r)^2+\Omega^2}\left(\frac{g^2}{\gamma^2+\Omega^2}\right)^n.$$

Binary Tree Haloscope

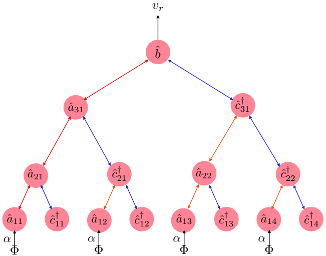

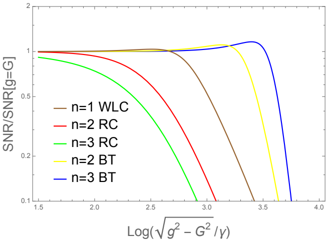

- **Fully $\mathcal{PT}$-symmetric setup** with $\hat{a}_{ij} \leftrightarrow \hat{c}^\dagger_{ij}$ brings strong **robustness**.
- Multi-probing sensors leads to **coherent enhancement**:

$$S^{\mathrm{BT}}_{\mathrm{sig}}(\Omega) = 2^{2n-2} S^{\mathrm{RC}}_{\mathrm{sig}}(\Omega).$$

Scalar Field Interferometry

Two point correlation function of the scalar field [Derevianko 18']:

$$\langle \Phi(0,\vec{0})\Phi(\tau,\vec{d})\rangle = \frac{\rho_\Phi}{\bar{\omega}} \int d^3\vec{v}\frac{f(\vec{v})}{\omega}\cos(\omega\tau - m_\Phi \vec{v}\cdot\vec{d}),$$

where $f(\vec{v}) \propto e^{-\frac{(\vec{v}-\vec{v}_g)^2}{2v_{\rm vir}^2}}$ and $\vec{v}_g$ is due to the Earth moving in the halo.

$$\text{Equal time } \tau = 0, \quad \langle \Phi(\vec{0})\Phi(\vec{d})\rangle \propto \exp\left(-\frac{d^2}{2\lambda_c^2}\right)\cos\left(m_\Phi \vec{v}_g\cdot\vec{d}\right).$$

- **Velocity fluctuation** $\sim v_{\rm vir}$ leads to **decoherence at dB length scale**.
- **Negative correlation** appears when $\vec{d}//\vec{v}_g$.

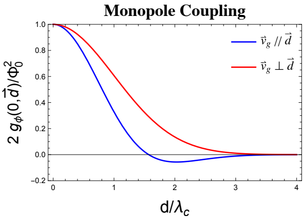

- **Daily modulation** due to the self-rotation of the Earth. [Foster, Kahn et al 20']

Axion Gradient and MDM Paraphoton

3×3 **matrix of dipole correlation**: $g(\tau, \vec{d})_{ij} \equiv \langle (\vec{\mathcal{O}}(t_1, \vec{x}_1) \cdot \vec{l}_i)(\vec{\mathcal{O}}(t_2, \vec{x}_2) \cdot \vec{l}_j) \rangle$.

- 5 possibilities when two $\vec{l}_i$ align:

$\vec{\mathcal{O}}^{\Phi} \propto \vec{v}$

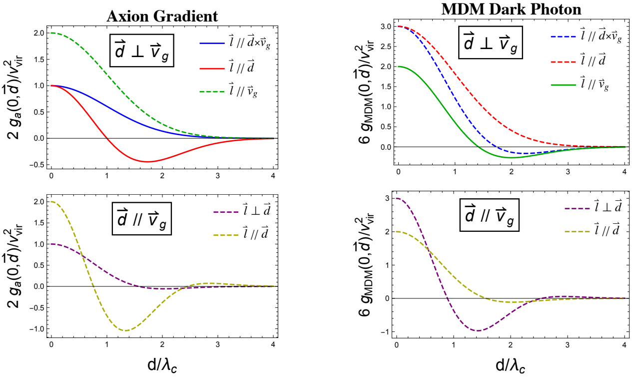

$\vec{\mathcal{O}}^{\mathrm{MDM}} \propto \vec{v} \times \hat{\epsilon}$

- **Straight lines** are not influenced by $\vec{v}_g$.
- Axion and MDM paraphoton **have totally different spatial correlations**.

Dipole Angular Correlation

Tune $\vec{l}_1$ and $\vec{l}_2$ with **certain directions at the same location**:

$$\Gamma(\vec{l}_1,\vec{l}_2) = \left(\vec{l}_1\right)^{\mathrm{T}}\cdot g(0,0)\cdot\vec{l}_2$$

$$= \begin{cases} \frac{v_{\mathrm{vir}}^2}{2}\,\vec{l}_1\cdot\vec{l}_2 + \frac{1}{2}\left(\vec{l}_1\cdot\vec{v}_g\right)\left(\vec{l}_2\cdot\vec{v}_g\right) & \text{Axion Gradient;} \\ \frac{v_{\mathrm{vir}}^2}{2}\,\vec{l}_1\cdot\vec{l}_2 - \frac{1}{6}\left(\vec{l}_1\cdot\vec{v}_g\right)\left(\vec{l}_2\cdot\vec{v}_g\right) & \text{MDM paraphoton;} \\ \frac{1}{6}\,\vec{l}_1\cdot\vec{l}_2 & \text{EDM paraphoton.} \end{cases}$$

- **Universal dipole angular correlation** $\vec{l}_1\cdot\vec{l}_2=\cos\theta$, in constrast with monopole or quadruple (H.D. curve) for stochastic GW searches.(LIGO, PTA).

  NANOGrav anomaly?

- $\vec{v}_g$ brings in anisotropy.

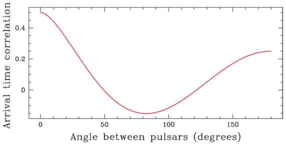

EDM, Kinetic Mixing and Hidden U(1) Dark Photon

3×3 matrix of dipole correlation: $g(\tau, \vec{d})_{ij} \equiv \langle (\vec{\mathcal{O}}(t_1, \vec{x_1}) \cdot \vec{l_i})(\vec{\mathcal{O}}(t_2, \vec{x_2}) \cdot \vec{l_j}) \rangle$.

- Each component of EDM paraphoton behaves the same with monopole since $\vec{\mathcal{O}}^{\mathrm{EDM}} \propto \hat{\epsilon}$.

- Other dipole sensors for dark photon:

  Kinetic mixing U(1) $\sim F_{\mu\nu} F'^{\mu\nu}$ with current $\vec{J}_{\mathrm{eff}} \propto \hat{\epsilon}$ in circuit or cavity detectors [Chaudhuri et al 15'];

  U(1) B-L & B with force $\vec{F} \propto \hat{\epsilon}$ in optomechanical detectors [Pierce Zhao et al 18' 20' 21'] or astrometry [Xiao et al 19' 21'].

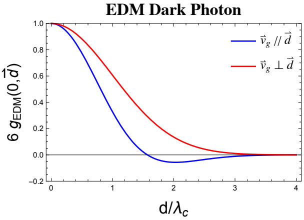

- Earth rotation needs to be taken into account when integration time is $> \mathcal{O}(1)$ day.

Higher Frequency Electromagnetic Resonant Detection

Difficult to detect $m_\Phi \gg$ GHz axion dark matter due to short λ_c.

I 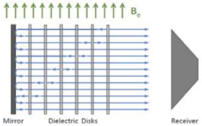

II 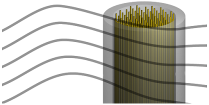

III 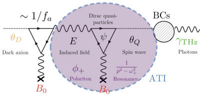

- I **Dielectric Haloscope**: discontinuity of E-field leads to coherent emission of photons from each surface, up to 50 GHz. [A.Caldwell et al 17']
- II **Plasma Haloscope**: using tunable cryogenic plasma to match axion mass, up to 100 GHz. [M.Lawson et al 19']
- III **Topological Insulator**: quasiparticle in it mixing with E field becomes polariton whose frequency can be tuned by magnetic field, up to THz. [D.J.E.Marsh et al 19']

Quantization of Cavity/Circuit Mode

- In Coulomb gauge, vector potential can be quantized

$$\vec{A}_k(\vec{r},t) = \sum_k \left(\frac{1}{2\omega_k}\right)^{1/2} \hat{a}_k u_k(\vec{r}) e^{-i\omega_k t} + h.c..$$

where $u_k(\vec{r})$ form a complete orthonormal set for a given boundary condition and $[\hat{a}_k, \hat{a}_{k'}] = \delta_{kk'}$.

- The Hamiltonian for each mode reduces to harmonic oscillator

$$H_{\rm cavity} = \frac{1}{2}\int \left(\vec{E}^2 + \vec{B}^2\right) d^3\vec{x} = \sum_k \omega_k \left(\hat{a}_k^\dagger \hat{a}_k + \frac{1}{2}\right).$$

- In the interaction picture, the coupling to axion is

$$H_{\rm int} = \int g_{\Phi\gamma} \Phi \vec{E}\cdot\vec{B}_0 d^3\vec{x} = \alpha\Phi(\hat{a}+\hat{a}^\dagger), \quad \alpha \simeq g_{\Phi\gamma} B_0 \sqrt{m_\Phi V}.$$

- Circuit mode can be quantized in the same way

$$H_{\rm LC} = \frac{\hat{Q}^2}{2C} + \frac{\hat{\phi}^2}{2L} = \omega_{\rm LC}\left(\hat{a}^\dagger \hat{a} + \frac{1}{2}\right).$$

Open quantum system

A quantum-mechanical system interacting with the environment:

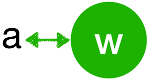

- System mode $\hat{a}$ couples to infinite degrees of freedom $\hat{w}_\omega$:

$$i\hbar\sqrt{2\gamma_r}\int_{-\infty}^{+\infty}\frac{d\omega}{2\pi}[\hat{a}^\dagger\hat{w}_\omega - \hat{a}\hat{w}_\omega^\dagger] + \int_{-\infty}^{+\infty}\frac{d\omega}{2\pi}\hbar\omega\hat{w}_\omega^\dagger\hat{w}_\omega.$$

- Fourier transformation: **0-dim localized mode** $\hat{a}$ couples to an 1-dim bulk w_ξ (transmission line):

$$i\hbar\sqrt{2\gamma_r}\hat{a}^\dagger\hat{w}_{\xi=0} + \mathrm{h.c.} + i\hbar\int_{-\infty}^{+\infty}d\xi\,\hat{w}_\xi^\dagger\partial_\xi\hat{w}_\xi.$$

- Equations of motion for $\hat{a}$ and outgoing mode $\hat{w}_{0_+}$:

$$\dot{\hat{a}} = -\gamma_r\hat{a} + \sqrt{2\gamma_r}\hat{w}_{0_-}; \qquad \hat{w}_{0_+} = \hat{w}_{0_-} - \sqrt{2\gamma_r}\hat{a}$$

Single Mode Resonator as Quantum Sensor

- For a resonator $\hat{a}$ **probing weak signal** Φ: $\alpha\left(\hat{a}+\hat{a}^{\dagger}\right)\Phi$
- Readout for outgoing mode $\hat{v}_r \equiv \hat{w}_{0_+}$:

$$\hat{v}_r = \frac{\Omega - i\gamma_r}{\Omega + i\gamma_r}\hat{u}_r + \frac{\sqrt{2\gamma_r}\alpha}{\Omega + i\gamma_r}\Phi.$$

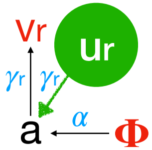

- Vacuum fluctuation in incoming mode $\hat{u}_r \equiv \hat{w}_{0_-}$ with white noise power spectral density $S_{\mathrm{r}} = 1$.
- Resonant signal spectrum $S_{\mathrm{sig}} = \frac{2\gamma_r\alpha^2}{\gamma_r^2+\Omega^2}\, S_{\Phi}(\Omega)$.

$$\text{Scan rate: } \int_{-\infty}^{+\infty} \frac{2\gamma_r\alpha^2}{\gamma_r^2+\Omega^2} d\Omega = \frac{\alpha^2}{2\pi}.$$

- Trade-off between peak sensitivity and bandwidth by tuning γ_r.

Intrinsic loss and fluctuation

- However, **intrinsic loss** proportional to γ exists, characterized by the quality factor $Q_{\rm int} \equiv \omega/\gamma$.

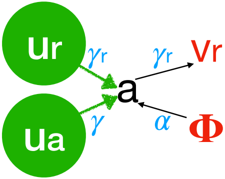

- According to the **fluctuation-dissipation theorem**, there is intrinsic noise $S_{\rm int}(\Omega) = \frac{4\gamma\gamma_r}{(\gamma+\gamma_r)^2+\Omega^2} S_{u_a}$ whose PSD contains both vacuum and thermal fluctuations:

$$S_{u_a} = n_{\rm occ} \equiv \left(\frac{1}{2} + \frac{1}{\exp\left(\omega/T\right) - 1}\right) \simeq \begin{cases} \frac{1}{2} & T \ll \omega; \\ \frac{T}{\omega} & T \gg \omega. \end{cases}$$

- **Standard quantum limit for power law detection: resonant $S_{\rm int}$+ flat $S_{\rm r}$**. [Chaudhuri et al 18']

Beam splitting coupling

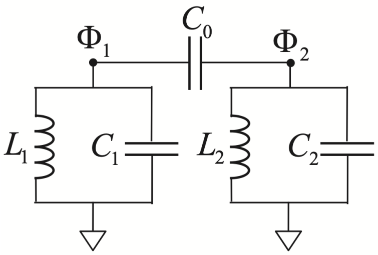

- Use an additional capacitor to couple two LC circuits:

$$H = \frac{1}{2}C_1\dot{\phi}_1^2 + \frac{1}{2}C_2\dot{\phi}_2^2 + \frac{1}{2L_1}\phi_1^2 + \frac{1}{2L_2}\phi_2^2 + \frac{1}{2}C_0(\dot{\phi}_1 - \dot{\phi}_2)^2.$$

- Conjugate momentum to ϕ_i involves mixing. Interaction potential:

$$\beta\hbar\sqrt{\omega_1\omega_2}(\hat{a}_1 - \hat{a}_1^\dagger)(\hat{a}_2 - \hat{a}_2^\dagger) \sim \hat{a}_1\hat{a}_2^\dagger + h.c.,$$

Non-Degenerate Parametric amplifier coupling

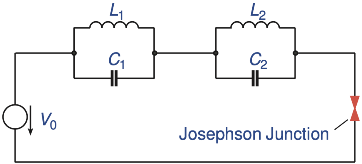

- Use a DC voltage and a Josephson junction to couple two LC circuits:

$$
\begin{aligned}
V &= -\frac{\hbar I_J}{2e_0}\cos\left(\omega_0 t + \frac{2e_0}{\hbar}(\phi_2+\phi_3)\right) \\
&= -\frac{\hbar I_J}{2e_0}\cos\left(\omega_0 t + \kappa_2(a_2+a_2^\dagger) + \kappa_3(a_3+a_3^\dagger)\right) \\
&\sim \frac{\hbar I_J}{4e_0}\kappa_2\kappa_3[a_2 a_3 + a_2^\dagger a_3^\dagger],
\end{aligned}
$$

Kinetic Mixing Dark Photon Dark Matter

- An additional $U(1)$ vector can have kinetic mixing with electromagnetic photon field through
$$\varepsilon F_{\mu\nu} F'^{\mu\nu}.$$
- It appears generally in theory with extra-dimension with a broad mass window predicted.
- Cold dark matter candidate behaving like **coherent wave**:

From Axion QED to Kinetic Mixing Dark Photon

$$\nabla \times \mathbf{B} = \partial_t \mathbf{E} + \mathbf{J} - g_{\Phi\gamma} \left(\mathbf{E} \times \nabla\Phi - \mathbf{B}\partial_t \Phi \right)$$

- Axion dark matter leads to an effective current under background $\mathbf{B}_0$ with $|J_{\rm eff}(t)| \sim g_{\Phi\gamma} B_0(t)\sqrt{\rho_{\rm DM}} \cos m_\Phi t$.

$$-\frac{1}{4}\left(\tilde{F}_{\mu\nu}\tilde{F}^{\mu\nu} + \tilde{F}'_{\mu\nu}\tilde{F}'^{\mu\nu}\right) + \frac{1}{2} m_{\gamma'}^2 \tilde{A}'_\mu \tilde{A}'^\mu - e J^\mu_{\rm EM} \tilde{A}_\mu + \varepsilon m_{\gamma'}^2 \tilde{A}_\mu \tilde{A}'^\mu.$$

- Similarly, in the interaction basis, the background dark photon behaves as an effective electromagnetic current with $J^\mu_{\rm eff} = \varepsilon m_{\gamma'}^2 \tilde{A}'^\mu$.

Effective current induced magnetic field

- In a space screened by electromagnetic shielding, the effective current can induce a transverse magnetic field
- For axion:

$$\begin{aligned} B_a &\approx |\vec{J}_a^{\mathrm{eff}}| \, V^{1/3}, \\ &\approx 10^{-17}\mathrm{T} \left(\frac{g_{a\gamma}}{10^{-11}\ \mathrm{GeV}^{-1}} \right) \left(\frac{B_0}{1\ \mathrm{T}} \right) \left(\frac{V^{1/3}}{1\ \mathrm{m}} \right) \end{aligned}$$

- For kinetic mixing dark photon (with a factor of 1/3 due to the isotropic wave-funtion):

$$\begin{aligned} B_{dp} &\approx |\vec{J}_{dp}^{\mathrm{eff}}| \, V^{1/3}, \\ &\approx 10^{-16}\mathrm{T} \left(\frac{\varepsilon}{10^{-6}} \right) \left(\frac{m_{dp}}{10\mathrm{Hz}} \right) \left(\frac{V^{1/3}}{1\ \mathrm{m}} \right). \end{aligned}$$

- V is the volume of the EM shielding room. Magnetic field signal is the strongest at the corner of the room.